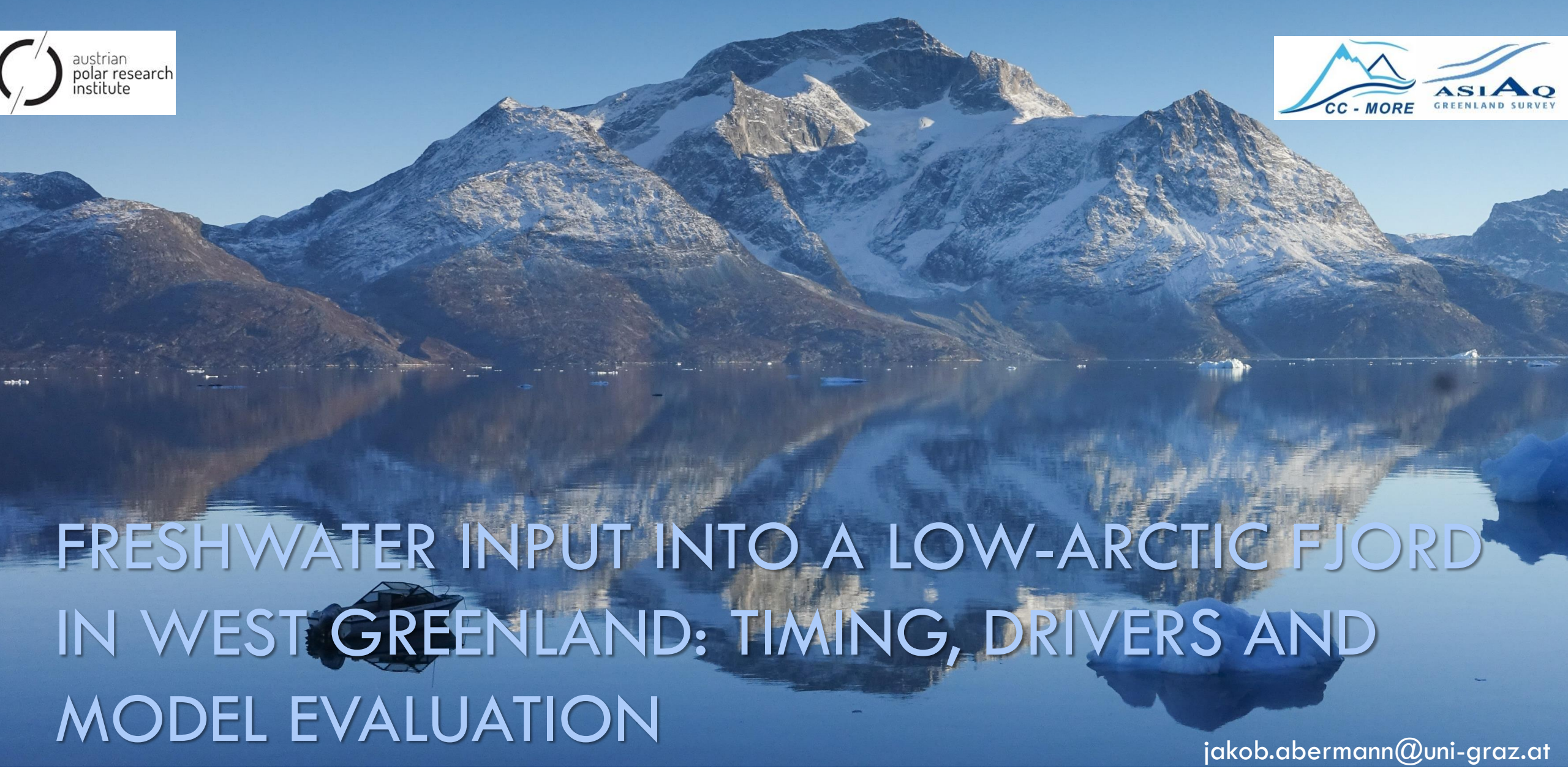

FRESHWATER INPUT INTO A LOW-ARCTIC FJORD IN WEST GREENLAND: TIMING, DRIVERS AND MODEL EVALUATION

jakob.abermann@uni-graz.at

Abermann, J.[1,2,3], Langley, K. [2], Myreng, S. [2], Petersen, D. [2], Rasmussen, K. [2], and Peßenteiner, S. [1]

[1]Department of Geography and Regional Science; University of Graz, Graz, Austria [2]Asiaq – Greenland Survey, Nuuk, Greenland; [3]Austrian Polar Research Institute, Vienna, Austra

Background

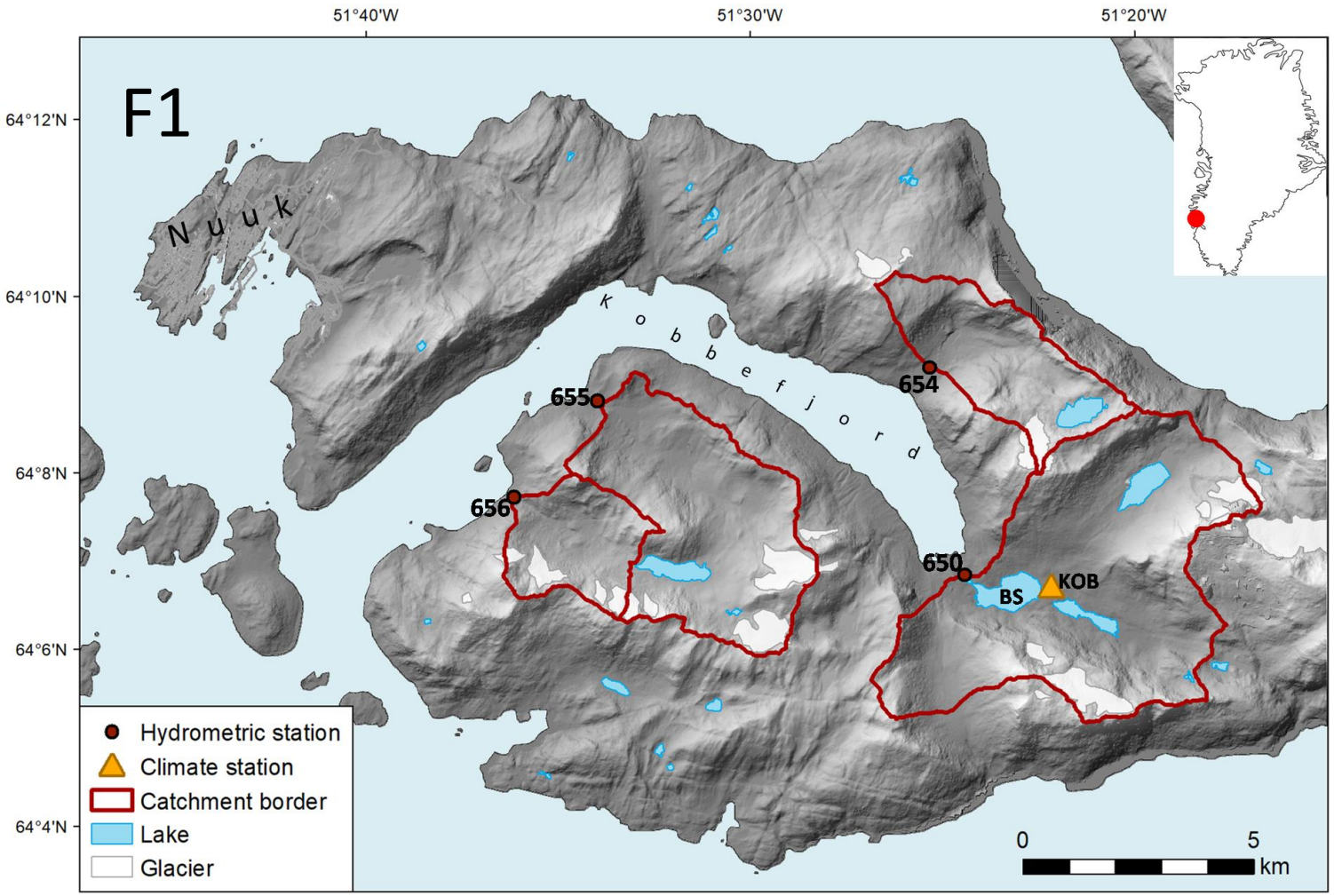

Fig. 1: The study area

About one quarter of the freshwater flowing from Greenland is derived from catchments that are disconnected from the Greenland Ice Sheet. Despite their importance to the total freshwater flux and their influence on fjord geochemistry, there is relatively little monitoring data available for those catchments and therefore the drivers of regional differences in export are largely unknown. We present a dataset of 12 years of discharge of four catchments less than 15 km apart, that are different in size (between 7 and 32 km²), local glacier coverage (4-11%) and lake cover (0-5%). They all drain into Kobbefjord, a well-studied fjord in West Greenland, near Greenland's capital Nuuk.

What makes the data presented in our study special is that we show four well-constrained and well-studied catchments in immediate vicinity with a rather similar climate driving the discharge dynamics. Through that we can explore differences in (I) annual totals, (II) seasonal cycle, (III) diurnal cycle and (IV) the drivers of these differences.

Catchment Characteristics

Figure 2 displays various catchment characteristics. Figure 2a shows the relative hypsometry of the individual catchments and significant differences can be seen across the catchments. The locations of the lakes (arrows) in 654, 655 and 650 are clearly associated with maxima of relative area coverage. Median elevation is highest at 654, lowest at 650 and almost equal at 655 and 656. Relative area distribution in the individual exposition segments is shown in Figure 2b. 655 and 656 have their main aspect towards the northern and eastern segments and 654 the largest parts directed between SE and SW. Figure 2c shows the relative distribution of slopes along with the median slopes for each catchment that is between 18° and 26°. 655 has large areas in very shallow slopes and the steepest catchments are 650 and 656. Potential solar radiation is shown in Figure 2d. Clearly, the largest average energy input throughout the year occurs at 654, and 656 receives the least, however, the individual catchments' maxima are within 10% of the highest potential incoming radiation.

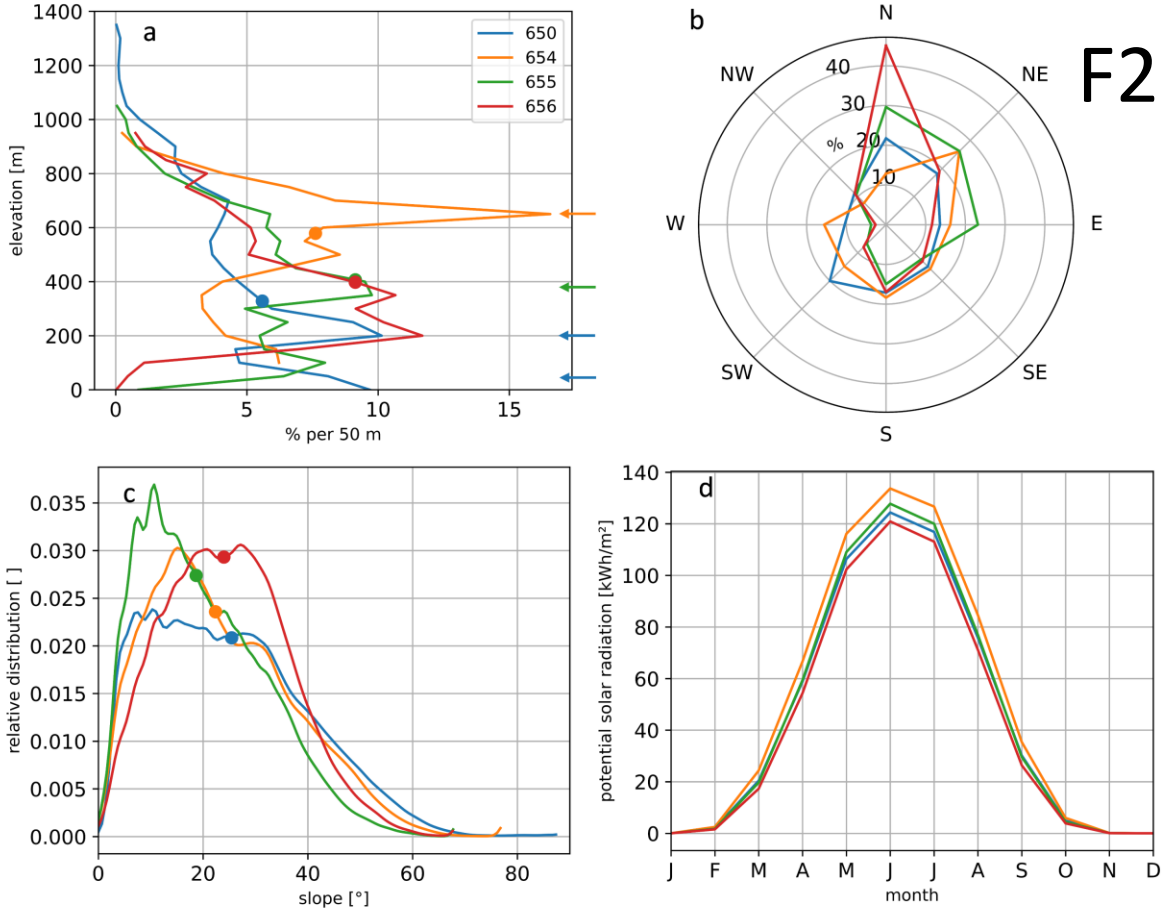

Fig. 2: Relative hypsometry of the studied catchments in 50 m bins based on the ArcticDEM; the respective median elevation is marked with a dot; heights above mean sea level are shown. The coloured arrows indicate the elevation in which a lake of a respective catchment is situated. Note, that the two lower lakes of catchment 650 are in the same elevation band, hence a single arrow indicates both those lakes. b) Polar diagram of each catchment's relative aspect distribution in % per aspect segment. The grouping was made in 45° increments around the 8 cardinal and intercardinal directions. 'NE' means for instance, that the respective area is directed towards NE, which is in this case the pixels with an azimuth of between 22.5° and 67.5°. c) Slope distribution [°]; the median slope is marked with a dot. d) Average potential solar incoming radiation [kWh/m²] for each catchment averaged for each month of the year

Specific Discharge

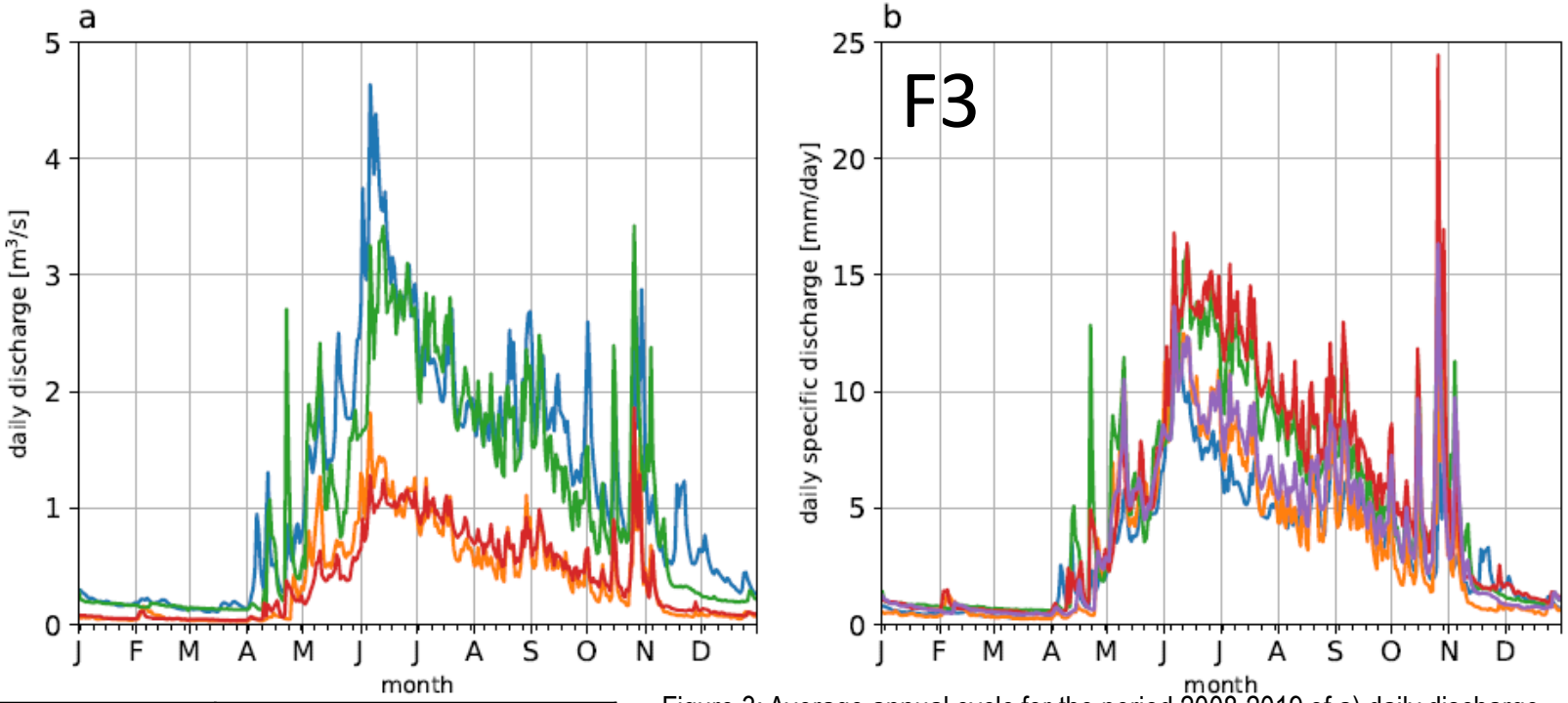

Figure 3: Average annual cycle for the period 2008-2019 of a) daily discharge [m³/s], b) daily specific discharge [mm]. Tab. 1 shows average specific discharge

Catchment	Average q [m/yr] 2008-2019 T1
650	1.18
654	1.21
655	1.74
656	1.87

Figure 3a shows the average annual cycle of daily mean discharge for each catchment. Until April very little water drains the catchments; thereafter a first peak comes with the onset of snowmelt. Summer and fall peaks are attributed to frontal activities leading to rain events. Absolute differences are largest between June and September. Daily averages reach more than 3 m3/s at 650 and 655 and remain much lower (around 1 m3/s) for most of the summer at 654 and 656 due to the smaller drainage areas. The absolute average contribution is higher at 654 than at 656 until early June while it is lower for the remainder of the year.

Figure 3b shows the average annual cycle of specific discharge in mm/day. Up until early June the four catchments show very similar values for baseflow conditions. Between June and late August there is a clear difference between the more exposed catchments (655 and 656) and the more continental, shaded catchments (650 and 654). This difference gets smaller towards the winter. In general, the highest absolute and specific discharge amounts are reached in early June. Spatial differences in specific discharge amount to up to 0.6 m/yr on average (Tab. 1).

Diurnal Cycle – ‘Fair Weather‘

We display the median relative diurnal cycle for May-August in Figure 4 for all days with both no precipitation and where the total incoming solar radiation for the respective day is within 80% of the maximum that has been measured at the site (14% of all days). With this filtering we intend to select sunny ‘fair weather days’ since they are expected to maintain a characteristic diurnal cycle and are per se independent of frontal activities. All gauges show a distinctive diurnal cycle. Among the stations there are significant differences: Strongest relative differences between morning and afternoon are at 654 in May and August and minimum and maximum are typically in the morning (8 AM) and the early evening (7 pm), respectively. From May to August, the maximum discharge at 650 is just after midnight and in the early morning hours and the minimum is just after noon in May and June and gets shifted to the evening hours in late summer. A difference in timing of maximum freshwater input into the fjord from the individual tributaries is thus up to 8-10 hours. For the total freshwater input from all four tributaries (purple curves in Figure 4) this results in a somewhat smoothed image that typically has its minimum in the late morning and maximum in the early evening, respectively. The time difference between maximum and minimum naturally changes with day length, which is most clearly visible for 654: While it is around 11 hours in June and July, there it is just 4-5 hours in September and October.

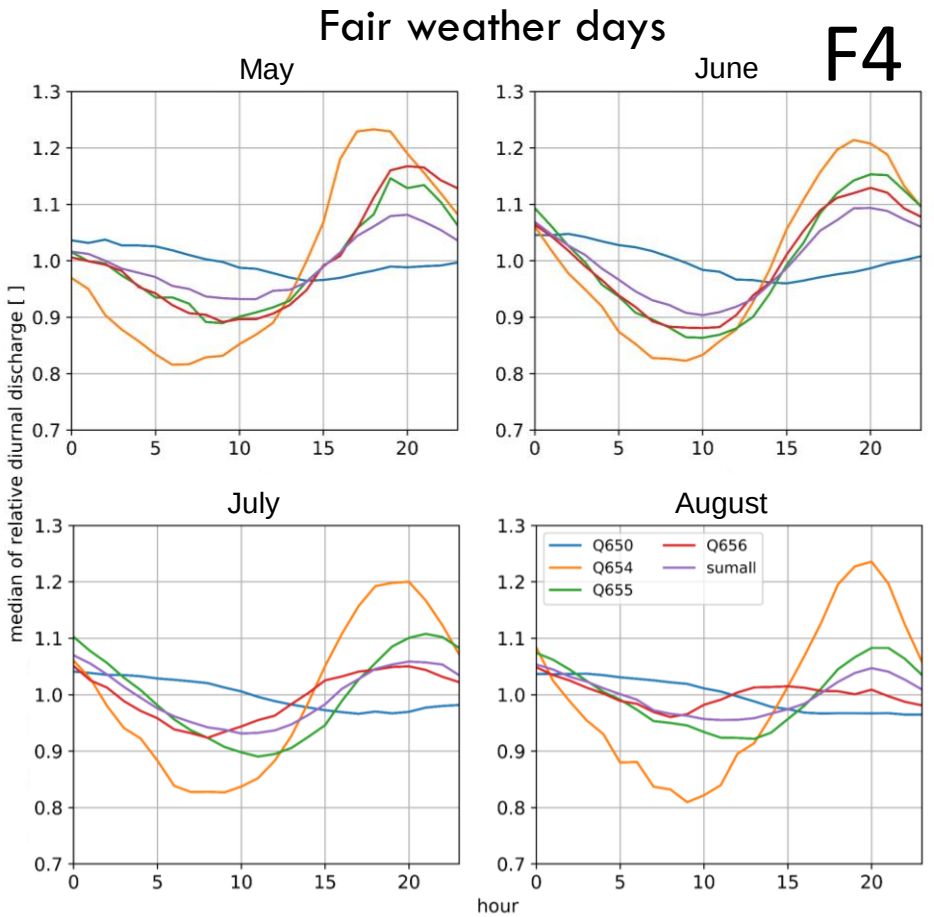

Figure 4: Monthly median diurnal cycle of relative hourly discharge for days without precipitation and solar radiation totals with more than 80% of the maximum daily solar incoming radiation at KOB for the respective day between 2008 and 2019.

Delay – ‘Fair Weather‘

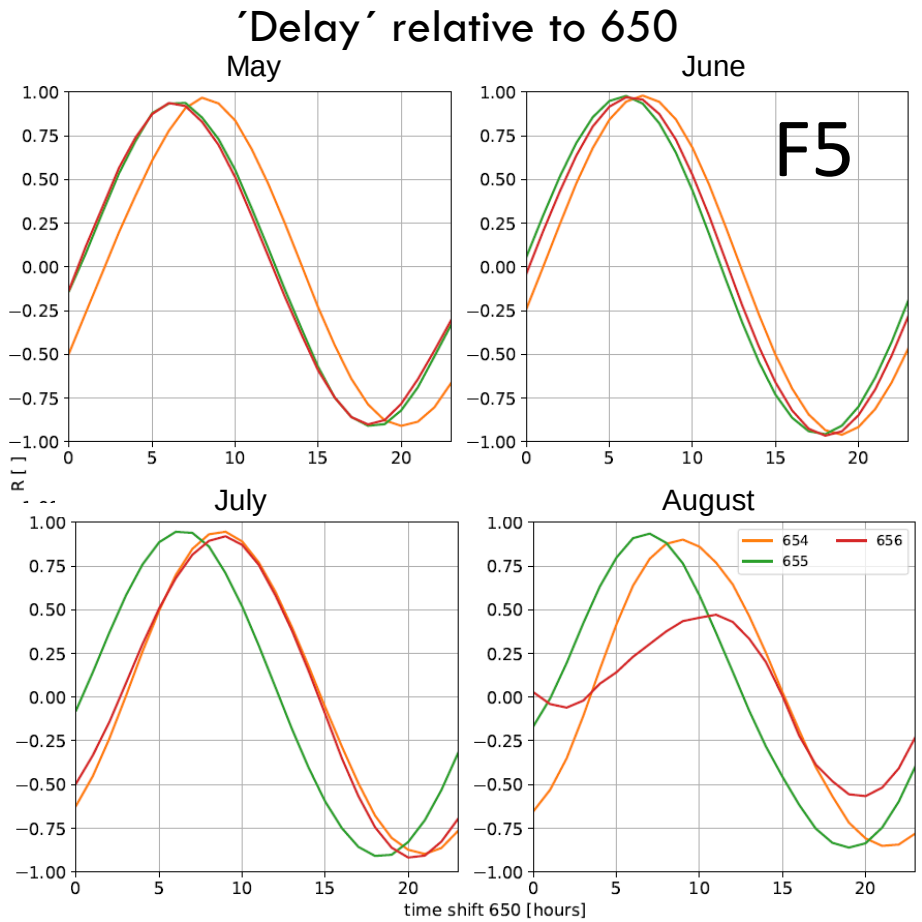

Figure 12: Pearson's correlation between 650 and the other catchments depending on a temporal cross-correlation of 650 for the months May to August for discharge during ‘fair-weather’ days. The maximum of R reflects the time lag of 650 relative to the respective station.

Overall, 650 reacts slower than the other three. It is an interesting problem to quantify the delay for the individual catchment which we attempt by deriving Pearson’s correlation of the median for both sets of cases as defined for Figure 4 (fair-weather days). We then shift the shape of 650 in hourly steps and derive correlations of the shifted cycle of 650 with each of the other catchments, referred to as ‘cross-correlation’ in the following. The highest value of the cross-correlation between the shifted 650 time series and the respective catchments can be interpreted as the delay of 650 relative to the respective station. The diurnal cycle for fair-weather cases is particularly notable for the summer months, which is why we show this analysis for May to August in Figure 5. We see a change throughout the summer season. Generally, 654 reacts fastest between May and July and the diurnal cycle of 650 has a typical time-lag of 7-8 hours compared to 654. This is a period when snowmelt controls discharge amounts particularly strongly at the radiation-exposed catchment 654. 650 is less delayed compared to 655 and 656 with seasonally rather stable 7 hours for 655. 656 shows the largest differences among the individual months: the cross-correlation reveals a delay of 650 of about 6 hours compared to 656 in the start of the melting season, while by August it is practically acyclic, i.e., around 12 hours. Correlation between 656 and 650 is also significantly weaker in this month, regardless of the shift – we attribute this to the glaciers as a more important driver of August discharge at 656.

Delay - precipitation

In order to assess how different the individual catchments react to a given precipitation event in terms of the timing of their freshwater input, we again make use of the hourly resolution of our data. We look at high discharge events and define them arbitrarily as containing at least one incident of 1 mm/hour specific discharge at 650. We use 650 as the arbitrary reference since we know that the other catchments react faster and thus earlier to precipitation. In Figure 6 we display the specific discharge of all these events (25 in total) relative to the maximum timing at 650. In addition, we show the total specific discharge and the cumulative precipitation related to the individual events. It is evident, that 654, 655 and 656 have the peak discharge around 8 hours earlier than 650. There is little difference between those three on average regarding timing as opposed to the difference in timing during fair-weather days. Cumulative precipitation at KOB indicates the strongest increase up until 5-8 hours before discharge peaks at 650, which is very close to the maximum specific discharge at 654, 655 and 656. Those catchments that have no lakes or with lakes in their higher part show thus a quicker reaction than 650, where storage in low-lying lakes occurs. Both variability and the magnitude of specific discharge are highest at 656, followed by 654 and 655.

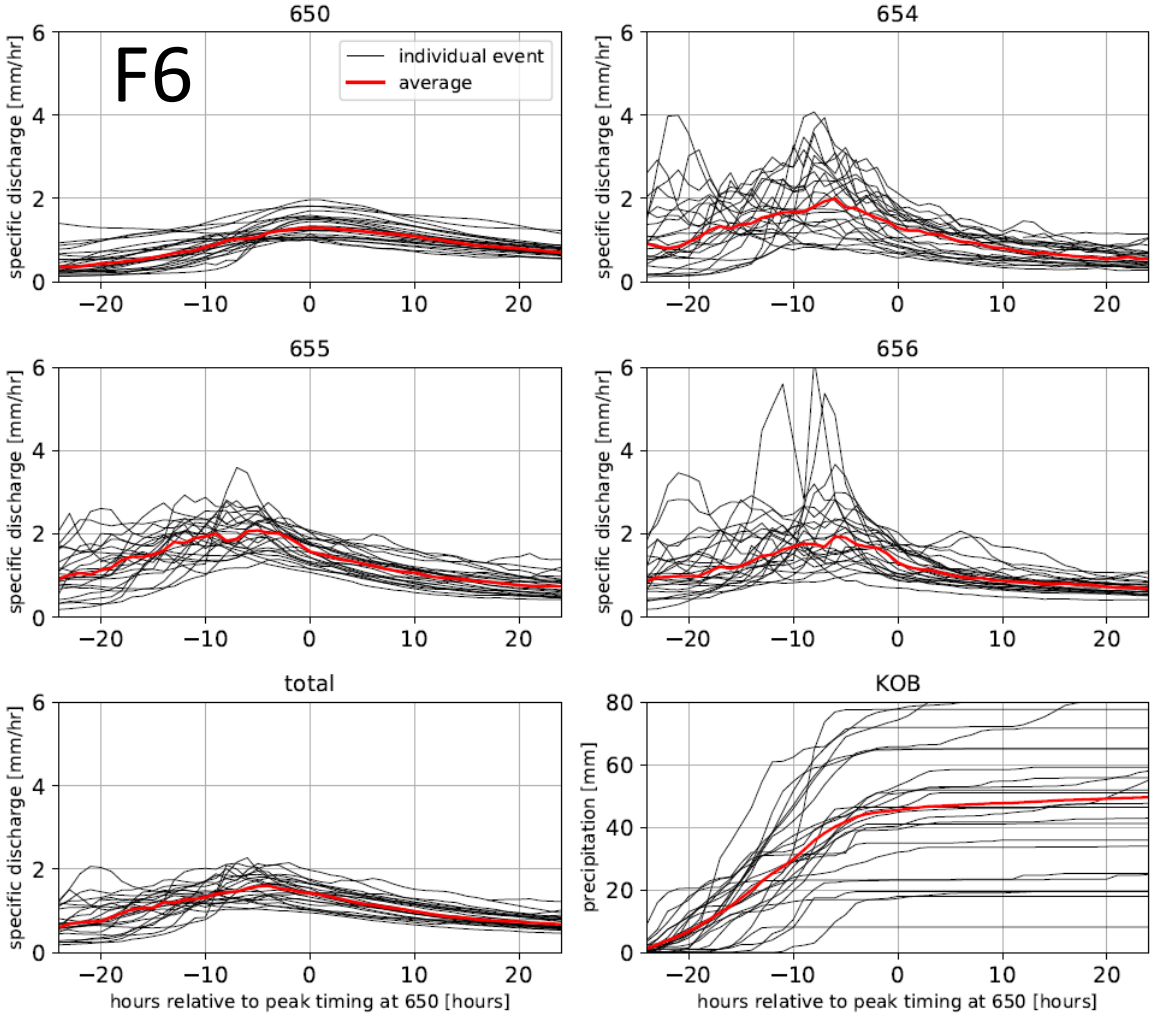

Figure 6: Specific discharge of all events that had at least one hour of 1 mm/hr specific discharge at 650. A time-scale relative to the maximum timing at 650 is shown in hours. Panels a-e show the sub-catchments and the specific discharge, while f shows the cumulative precipitation at KOB starting 24 hours before the maximum at 650 until 24 hours after the maximum at 650.

Model validation

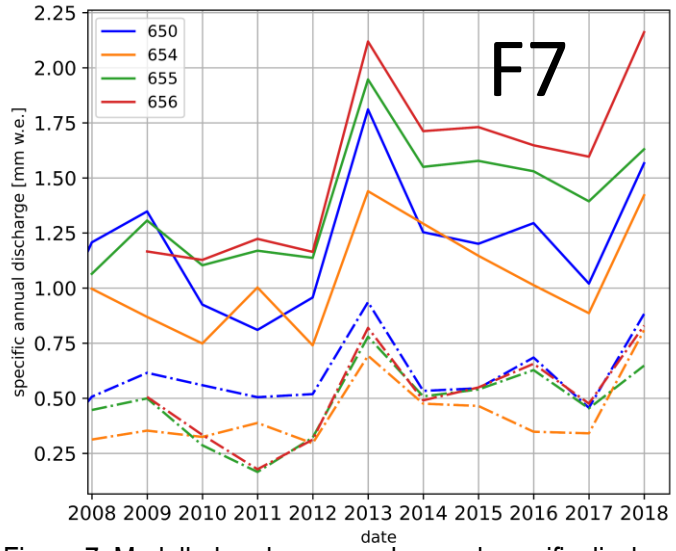

Figure 7: Modelled and measured annual specific discharge

A recent modelling study (Mankoff et al. 2020) provides diurnal discharge for all catchments in Greenland based on RCM output. Fig. 7 shows annual specific discharge totals measured (solid) and modelled (dashed). While the variability is reproduced, the absolute values are significantly underestimated and the spatial gradients are poorly captured. Fig. 8 shows daily discharge values (measured vs. modelled) for each catchment and Tab. 2 displays the respective Nash-Sutcliffe Efficiency. Values between -0.51 and 0.31 show a rather poor model performance. Exemplarily, daily discharge values are shown for 2017 in Fig 9. Early spring discharge is captured well as is the timing of individual peak-flow events. The overall underestimation of the model is likely related to a strong underestimation of base-flow. We are currently applying a process-based calibrated discharge model (WaSim) in order to build a basis for sensitivity studies and climate change scenario modelling. Also, ML approaches will be explored in order to assess the potential for improving the existing modelling results.

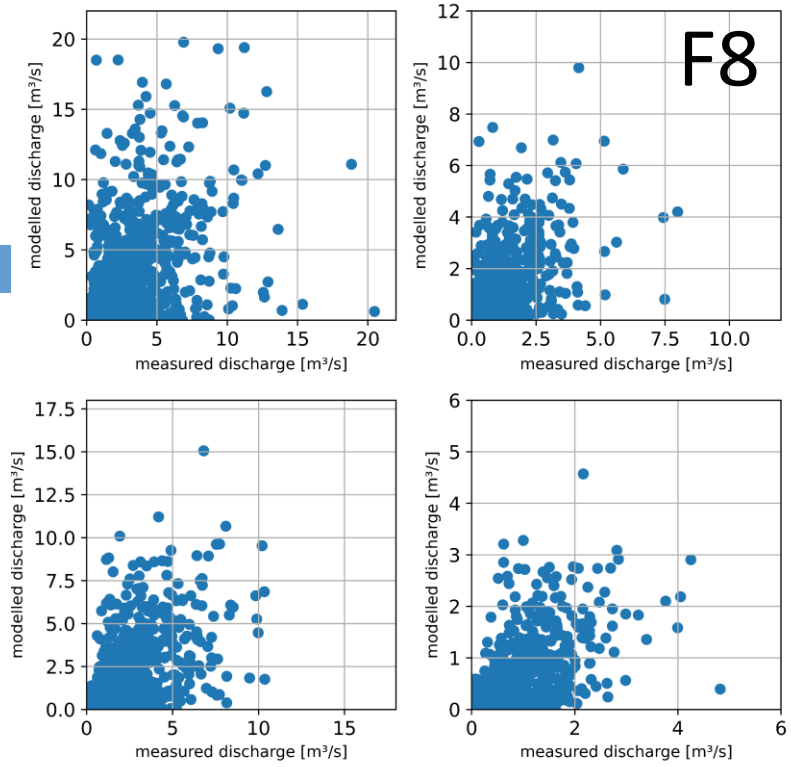

Figure 8: Modelled and measured daily discharge in 2017

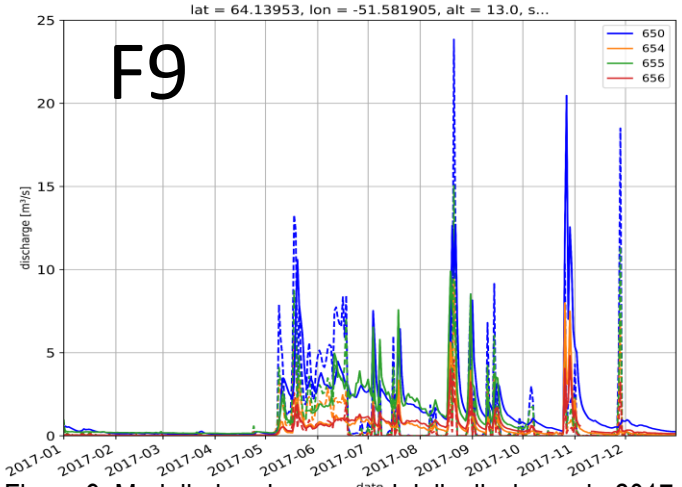

Figure 9: Modelled and measured daily discharge in 2017

Station	NSE [ ]
650	0.24
654	0.31
655	-0.02
656	-0.51

T2

Tabel 2: Nash-Sutcliffe Efficency f
daily values of modelled v
measured discharge.

Summary

- Within <15 km
  - climatological specific discharge differs by 0.6 m/a
    - Precipitation gradients
  - diurnal cycle differs by 6-11 hours
    - Snow melt
    - Catchment characteristics
  - Flood peak discharge differs less but also significantly
    - Buffering effects by lakes
- Existing model captures variability but highly underestimates total discharge
- > 30.000 land basins in Greenland
- Implication for upscaling

References

Abermann, J., K. Langley, S. Myreng, D. Petersen, K. Rasmussen (submitted to Hydr. Proc.): Heterogeneous timing of freshwater input into Kobbefjord, a low-Arctic Fjord in Greenland. Hallouin, T. (2021). HydroEval: Streamflow Simulations Evaluator (Version 0.1.0). Zenodo. https://doi.org/10.5281/zenodo.2591217

Mankoff, K. D., Ahlstrøm, A. P., Colgan, W., Fausto, R. S., Fettweis, X., Kondo, K., Langley, K., Noël, B., Sugiyama, S. and van As, D.: Greenland liquid water runoff from 1979 through 2017, Earth Syst. Sci. Data Discuss., (April), 1–44, doi:https://doi.org/10.5194/essd-2020-47, 2020.

Nash, J. E. and Sutcliffe, J. V: River flow forecasting through conceptual models part {I} — {A} discussion of principles, J. Hydrol., 10(3), 282–290, doi:10.1016/0022-1694(70)90255-6, 1970.

http://www.wasim.ch/downloads/doku/wasim/wasim_2012_ed2_en.pdf